Fast and Stable Topology Optimization of Motors Considering Iron Losses

Shintaro Furui†, Ting Fu† and Hajime Igarashi†

†Graduate School of Information Science and Technology, Hokkaido University
Sapporo, Hokkaido 060-0814, JAPAN
Email: sfurui@em.ist.hokudai.ac.jp, futing@em.ist.hokudai.ac.jp, igarashi@ssi.ist.hokudai.ac.jp

Abstract– This paper presents a fast and stable topology optimization method based on normalized Gaussian network. The novelty of the proposed method is to control smoothness of the device shapes obtained by the topology optimization. In this method, a regularization term which characterizes the spatial change near the shape boundaries is introduced. The proposed method is applied to optimization of a magnetic shield and synchronous reluctance motor. The optimization result shows that the present method results in smooth optimal shapes with satisfactory performance.

1. Introduction

Synchronous reluctance motor (SynRM) has attained attentions because of its simple rotor structure without permanent magnets and high torque density. It has widely been used for, e.g., elevators and robots [1]. For this reason, there have been many studies on optimization of the SynRM [2, 3]. To find novel optimal rotor shapes of SynRM, topology optimization methods would be effective [4]-[6].

There are two major topology optimization methods: level-set based and on/off-based method. In the former method, material shapes are represented by contour lines of an implicit function called level-set function. This method advantageously results in smooth material boundaries [7, 8]. Moreover, it has relatively low computational cost because optimization is performed by gradient methods. The objective and restriction functions must be, therefore, differentiable and the optimization results highly depend on the initial solution.

In the latter method, the on/off states of small cells are optimized by the metaheuristic algorithm such as genetic algorithm (GA). This method can alleviate the above mentioned difficulties of the level-set method. However, the resultant shapes tend to be complicated because of its high degree of freedom. To avoid this problem, on/off states have been determined from the levels of normalized Gaussian network (NGnet) [9]. This method has been successfully applied to optimization of the rotor shape of SynRM [2]. However, this method does not always result in smooth material boundaries.

We have proposed a method to control smoothness of material boundaries obtained by the NGnet-based method [10]. However, validity of this method for optimization of SynRM remains unclear. In this paper, we discuss the performance of this method applied to optimization of rotor shapes of SynRM considering iron losses.

2. Optimization method

In this method, the on/off status of each element is determined from the output of NGnet $\phi(\boldsymbol{x}_e)$ given by

$$\phi(\boldsymbol{x}_e) = \sum_{i=1}^{N_g} w_i b_i(\boldsymbol{x}_e) \tag{1}$$

$$b_i(\boldsymbol{x}_e) = \frac{G_i(\boldsymbol{x}_e)}{\sum_{j=1}^{N_g} G_j(\boldsymbol{x}_e)} \tag{2}$$

where $\boldsymbol{x}_e$, G_i, w_i and N_g are the center of finite element e, Gaussian function, weighting coefficient and the number of the Gaussian functions. When the value of w_i is given, the state V_e of element e is determined from

$$V_e \leftarrow \begin{cases} on & \phi(\boldsymbol{x}_e) \geq 0, \\ off & \phi(\boldsymbol{x}_e) < 0. \end{cases} \tag{3}$$

If V_e is *on* (*off*), the material property of V_e is set to magnetic material (air). In the optimization process, w_i is optimized by using real-coded GA to minimize objective function. An example of the material boundary determined from NGnet is shown in Fig.1, where w_i is set to {0.5, -0.5}.

To control smoothness of the material boundaries, the objective function f is modified by introducing the regularization term as follows:

$$F = f + k\int \left|\nabla \tanh(\alpha\phi(\boldsymbol{x}_e))\right|^2 \mathrm{d}S \tag{4}$$

Note that the integrand becomes large only near the material boundaries.

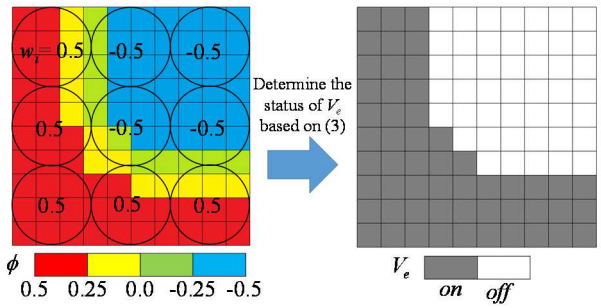

Fig. 1 Determination of material boundary

3. Optimization results

To examine the validity of the present method, we apply it to optimization of a magnetic shield and then rotor structure of the SynRM.

3.1. Magnetic Shield

The optimization model is shown in Fig. 2 [11]. This model is axisymmetric and the number of nodes and finite elements are 101441 and 100800. The relative permeability of the magnetic material is set to 1000. The goal of this optimization is to minimize the flux density B in the target region as well as to minimize the volume of magnetic material V. The optimization problem is defined by

$$F = \frac{B}{B_{\mathrm{T}}} + \frac{V}{V_{\mathrm{T}}} + k \int_{\Omega_{\mathrm{d}}} \left| \nabla \tanh(\alpha\phi) \right|^2 \mathrm{d}S \rightarrow \min., \qquad (5)$$

where the normalization constants are set as follows: B_{T}=5.0 μT, V_{T}=1.07 cm^3. In this optimization, α is set to 10 and 75 Gaussian bases are deployed uniformly in the design region Ω_{d} as shown in Fig. 3.

Fig. 4 shows the resultant shapes and flux lines. When there is no regularization term, the shield shape is found rather complicated. In addition, there is a small magnetic island. On the other hand, when the regularization term is introduced, the smooth-shaped double shielding structure is obtained.

The distribution of $|\nabla\tanh(\alpha\phi)|$ is shown in Fig. 5. The regions where $|\nabla\tanh(\alpha\phi)|$ takes large values localize near the material boundaries in Fig.5 (a). On the other hand, the distribution of $|\nabla\tanh(\alpha\phi)|$ is rather uniform in Fig. 5 (b).

The convergence history of GA is shown in Fig. 6. Introduction of the normalization term leads to better convergence. This suggests that the present method can accelerate the optimization process.

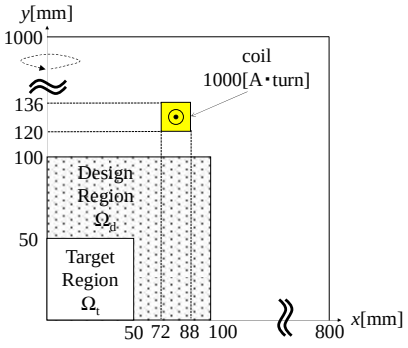

Fig. 2 Magnetic shield model

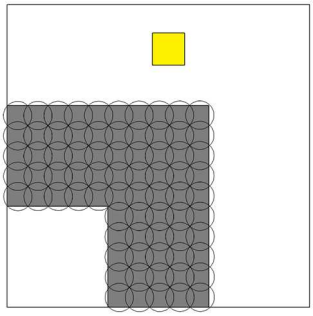

Fig. 3 Deployment of Gaussian

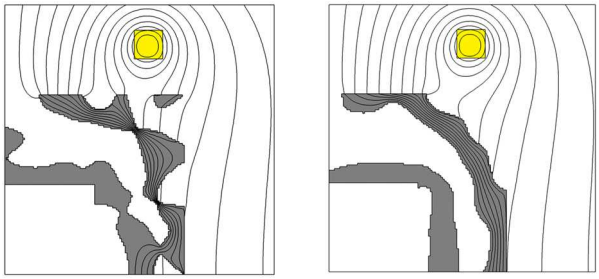

B=7.67 μT, V=1.29 cm^3 (a) k=0.0 B=1.12 μT, V=1.18 cm^3 (b) k=1.0×10^{-3}

Fig. 4 Optimized shapes and flux lines of magnetic shield

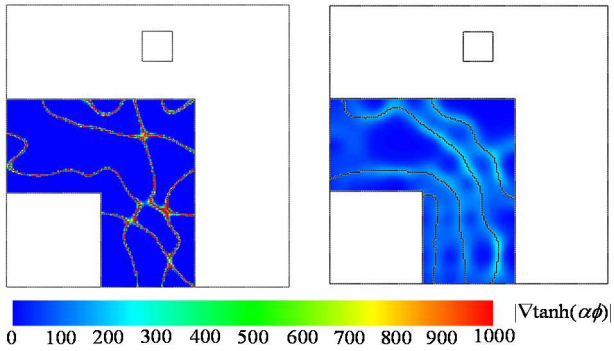

(a) k=0.0 (b) k=1.0×10^{-3}

Fig. 5 Distribution of $|\nabla\tanh(\alpha\phi)|$

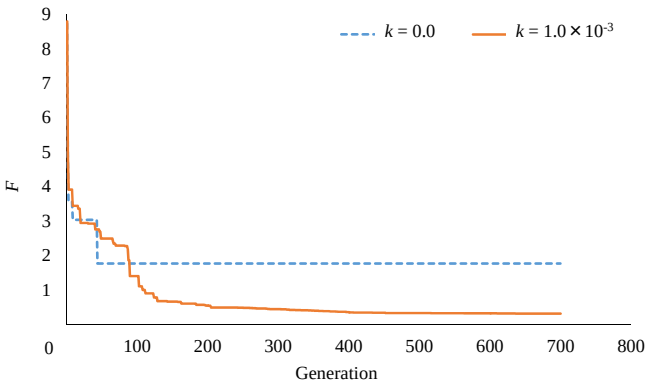

Fig. 6 Convergence history of GA

3.2. SynRM

The optimization model of SynRM is shown in Fig. 7. The design region of this model is 1/8 of the rotor because of its symmetry. The number of nodes and finite elements are 13971 and 13628.

To evaluate iron loss in the SynRM, we employ 1D method [12] in which the magnetic vector potential distribution in an electrical steel sheet is evaluated in the post processing of the 2-D FE analysis. In this method, electromagnetic fields in a steel sheet are determined by solving 1-D equation of quasi-static electromagnetic field. The iron loss which is composed of eddy current and hysteresis loss is calculated from the resultant vector potential.

To evaluate iron loss in the stator of 4-pole SynRM accurately, we have to perform the 2-D FE analysis at fine angular pitch ranging from 0 to 180 degrees because of the cycle of the flux density in the stator core. Because it takes long computational time, this fine analysis would be unsuitable for the optimization processes. For this reasons, we perform the 2-D FE analysis at 5 degree intervals in the optimization process. In the post process, the field analysis is performed at 1 degree intervals.

The Gaussian bases are uniformly distributed in the design region as shown in Fig. 8. The analysis condition and specifications are summarized in Table I. In this optimization, the core material is assumed to be 50A470.

The goal of this optimization is to minimize the iron loss W_{loss} in the rotor and stator core keeping the average torque T_{ave} higher than $0.8T_{\text{ref}}$ where T_{ref} is the average torque of reference model shown in Fig. 9, which is obtained by the parameter optimization. The optimization problem is defined by

$$F = \frac{W_{\text{loss}}}{W_{\text{ref}}} + k \int_{\Omega_D} \left|\nabla \tanh(\alpha\phi)\right|^2 \mathrm{d}S \rightarrow \min., \tag{6}$$

$$\text{sub.to} \quad T_{\text{ave}} > 0.8T_{\text{ref}}, \quad N_{\text{area}} < 2 \tag{7}$$

where the normalization constants are set as follows: W_{ref}=7.19 W and T_{ref}=2.32 Nm, which correspond to the iron loss and the average torque of the reference model. Furthermore, N_{area} is the number of isolated iron cores. In this optimization, α is set to 10 again.

Fig. 10 shows the resultant shapes and flux lines. The iron loss in both optimal shapes are smaller than that of the reference model. The reason why the iron loss of the optimal shapes is reduced is that magnetic material near the surface of the rotor core in which iron loss concentrates is scraped off. The average torque in Fig. 10 (a), which is computed in the post processing, violates restriction (7) because the field computation is performed at 5 degrees intervals in the optimization process. The material boundary in Fig. 10 (b) has simpler shape than that of (a).

The distribution of $|\nabla\tanh(\alpha\phi)|$ is shown in Fig. 11. The tendencies in the distributions are similar to those of the magnetic shield problem shown in Fig. 5. Fig. 12 shows distribution of iron loss density. The iron loss is suppressed small near the rotor surface in Fig. 12 (a) while it is rather uniform in (b).

The convergence history of GA is shown in Fig. 13. It is found again that introduction of the regularization term accelerates convergence.

Table I
Analysis conditions and specifications

Rotation speed [rpm]	1500
Current amplitude [A]	8.48
Number of turns [turn]	35
Current phase angle [degree]	45

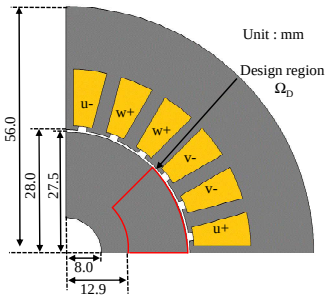

Fig. 7 SynRM model

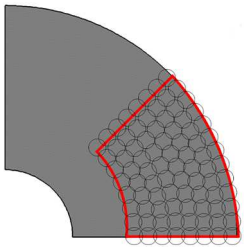
Fig. 8 Deployment of Gaussian

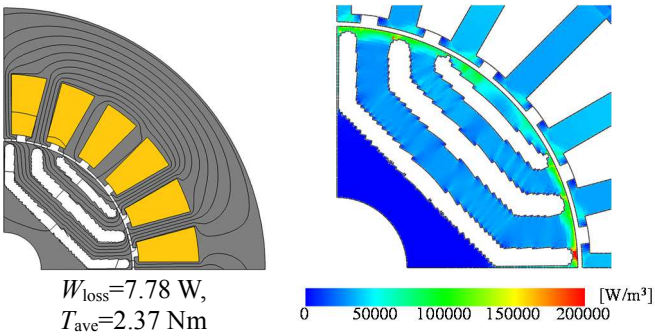

W_{loss}=7.78 W, T_{ave}=2.37 Nm
(a) Shape and flux lines (b) Iron loss density distribution
Fig. 9 Reference SynRM model [3]

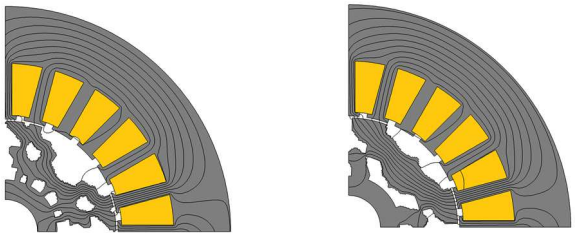
W_{loss}=6.75 W, T_{ave}=1.71 Nm, (a) $k = 0.0$
W_{loss}=7.01 W, T_{ave}=1.90 Nm (b) $k = 5.0\times10^{-3}$
Fig. 10 Optimized shapes and flux lines of SynRM

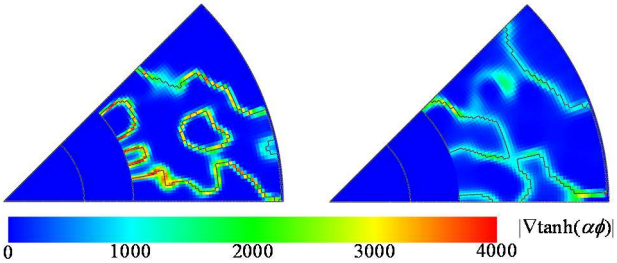

(a) $k = 0.0$ (b) $k = 5.0\times10^{-3}$
Fig. 11 Distribution of $|\nabla\tanh(\alpha\phi)|$ in the design region

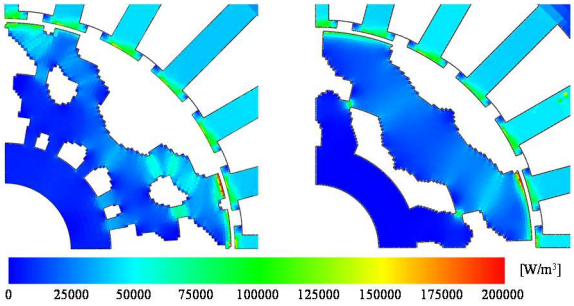

(a) $k = 0.0$ (b) $k = 5.0 \times 10^{-3}$

Fig. 12 Distribution of iron loss density

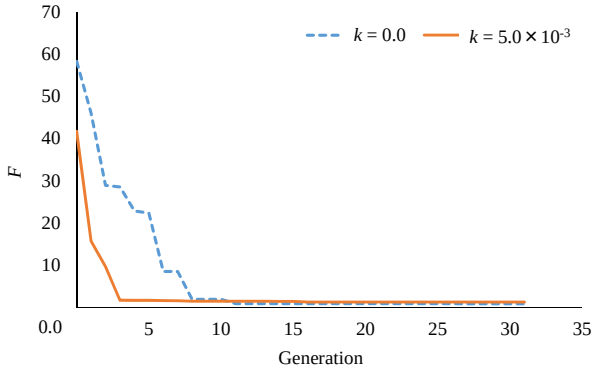

Fig. 13 Convergence history of GA

4. Conclusion

In this paper, we have discussed the topology optimization method based on NGnet in which the regularization term is introduced to control smothness of material boundaries. The shapes of magnetic shield and SynRM are successfully optimized by the present method. It has been found that introduction of the regularization term does not only make the material boundaries smoother but also improves convergence of GA processes. The determination of suitable values of k is remained for future work.

Acknowledgments

This work was supported in part by JSPS KAKENHI Grant Number 25630101.

References

[1] J. Soltani and H. A. Zarchi, "Robust optimal speed tracking control of a current sensorless reluctance motor drive using a new sliding mode controller," *Power Electronics and Drive Systems*, *2003*. *PEDS 2003*. Vol. 1, pp.474-479, 2003.

[2] S. Sato, T. Sato, H. Igarashi, "Topology optimization of Synchronous reluctance motor using normalized Gaussian network," *IEEE Trans*, *Magnetics*, vol. 51, no. 3, 2015.

[3] G. Pellegrino, F. Cupertino and C. Gerada, "Barriers shapes and minimum set of rotor parameters in the automated design of Synchronous Reluctance machines," *Proc. Of IEMDC2013*, pp.1204-1210, 2013.

[4] Y. Hidaka, S. Furui and H. Igarashi, "Robust Optimization Considering Probabilistic magnetic degradation," *IEEE Trans*, *Magnetics*, vol. 51, no. 3, 2015.

[5] D. H. Kim, I. Park, J. H. Lee and C. E. Kim, "Optimal shape design of iron core to reduce cogging torque of IPM motor." *IEEE Trans*, *Magnetics*, vol. 39, no. 3, 2003.

[6] N. Takahashi, T. Yamada, S. Shimose and D. Miyagi, "Optimization of rotor of actual IPM motor using ON/OFF method," *IEEE Trans*, *Magnetics*, vol. 47, no. 5, pp.1262-1265, 2011.

[7] Y. Hidaka, T. Sato, H. Igarashi, "Topology Optimization Method Based on On-Off Method and Level Set Approach." *IEEE Trans*, *Magnetics*, vol. 50, no.2, pp. 617-620, 2014.

[8] T. Yamada, K. Izui, S. Nishiwaki and A. Takezawa, "A topology optimization method based on the level set method incorporating a fictitious interface energy," *Computer Methods in Applied Mechanics and Engineering*, vol. 199, no. 45, pp. 2876-2891, 2010.

[9] T. Sato, K. Watanabe, and H. Igarashi, "Multimaterial Topology Optimization of Electric Machines Based on Normalized Gaussian Network," *IEEE Trans. Magnetics*, vol. 51, no. 3, 2015.

[10] S. Furui, S. Sato, T. Sato and H. Igarashi, "Topology Optimization of IPM Motors to Minimize Iron Losses," *IEEE Trans*. *Magnetics*, to be submitted.

[11] Y. Tominaga, Y. Okamoto and S. Sato, "Optimal Topology Design for Magnetic Shielding Using Multistep Genetic Algorithm," Joint Technical Meeting on Static Apparatus and Rotating Machinery, IEE Japan, SA-11-49, RM-11-49, pp.17-22, 2011.

[12] K. Yamazaki and N. Fukushima, "Torque and loss calculation of rotating machines considering laminated cores using post 1-D analysis," *IEEE Trans*. *Magnetics*, vol. 47, no. 5, pp.994-997, 2011.